

Synthesis and Structure of Tetra(*para*-tolyl)antimony Dicyanodiidoaurate [*p*-Tol₄Sb][Au(CN)₂I₂] and Alkyltriphenylphosphonium Dicyanodiidoaurates [Ph₃PAalk][Au(CN)₂I₂], Alk = Me, CH₂CN

V. V. Sharutin^a, O. K. Sharutina^a, A. N. Efremov^{a, *}, and O. S. Eltsov^b

^aNational South Ural State Research University, Chelyabinsk, 454080 Russia

^bUral Federal University Named after the First President of Russia B.N. Yeltsin, Yekaterinburg, 620002 Russia

*e-mail: efremov_an94@mail.ru

Received November 26, 2019; revised February 10, 2020; accepted March 11, 2020

Abstract—Red-colored crystalline gold complexes [*p*-Tol₄Sb][Au(CN)₂I₂] (**I**), [Ph₃PMe][Au(CN)₂I₂] (**II**), and [Ph₃PCH₂CN][Au(CN)₂I₂] (**III**) were synthesized by the reaction of potassium dicyanodiidoaurate with tetra(*para*-tolyl)antimony and alkyltriphenylphosphonium halides in water. The structure of the complexes was established by IR and NMR spectroscopy and X-ray diffraction. The tetra(*para*-tolyl)antimony and alkyltriphenylphosphonium cations have a distorted tetrahedral coordination. The dicyanodiidoaurate anions have a planar structure with a square coordination of the gold atom. The formation of the 3D crystal network is due to weak CN···H–C hydrogen bonds between cations and anions (2.39, 2.59 Å (**I**), 2.70, 2.48, 2.52, 2.68 Å (**II**), 2.73, 2.50, 2.67, 2.44 Å (**III**)). In complex **III**, anions of one of the two types interact with one another via I···I contacts to give 1D ladder-like chains along the crystallographic *a* axis.

Keywords: potassium dicyanodiidoaurate, tetra(*para*-tolyl)antimony dicyanodiidoaurate, methyltriphenylphosphonium dicyanodiidoaurate, cyanomethyltriphenylphosphonium dicyanodiidoaurate, X-ray diffraction analysis

DOI: 10.1134/S1070328420090031

INTRODUCTION

The attention of researchers to gold dicyanide complexes is caused by their application for the manufacture of materials with various photochemical and photophysical properties [1–8]. They were shown to be active metabolites of certain drugs [9]. The [Au(CN)₂][–] anions can form polymer and oligomer frameworks possessing luminescent properties [4, 5, 8–11]. Gold(III) cyano halide complexes are used as sensors for volatile organic compounds (DMF, dioxane, pyridine, ethylene glycol) [12] and as precursors for dicyanide synthesis [13]. Currently, several gold(I) cyanide complexes [14–16] and gold(III) cyano halide complexes with organic and inorganic cations [12, 13, 17–20] are known; however, complexes [Cat]⁺[Au(CN)₂Hal₂][–] with organoelement cations have not been studied.

For elucidating the details of synthesis and structure of tetraarylantimony and tetraorganylphosphonium dicyanodiidoaurate complexes, here we synthesized and structurally characterized for the first time tetra(*para*-tolyl)antimony dicyanodiidoaurate [*p*-Tol₄Sb][Au(CN)₂I₂] (**I**) and alkyltriphenylphos-

phonium dicyanodiidoaurates [Ph₃PAalk][Au(CN)₂I₂], Alk = Me (**II**), CH₂CN (**III**).

EXPERIMENTAL

Synthesis of tetra(*para*-tolyl)antimony dicyanodiidoaurate (I**).** A solution of potassium dicyanodiidoaurate (104 mg, 0.192 mmol) in water (5 mL) was added to a solution of tetra(*para*-tolyl)antimony chloride (100 mg, 0.192 mmol) in water (10 mL), and the mixture was stirred and kept at 20°C for 14 h. After evaporation of water, the solid residue was dried and recrystallized from an acetonitrile–ethanol solvent mixture (2 : 1 v/v). On slow evaporation of the solvent, red crystals formed. The yield of **I** was 179 mg (94%). *T*_{dec.} = 161°C.

IR (ν, cm^{–1}): 3047, 3020, 2980, 2916, 2862, 2166, 2156, 1913, 1643, 1589, 1492, 1442, 1396, 1317, 1211, 1190, 1118, 1068, 1039, 1012, 848, 796, 696, 632, 584, 480, 439, 430.

¹H NMR (DMSO-d₆; 600 MHz; δ, ppm): 2.41 (s, 12H, –CH₃), 7.48 (d, 8H, arom. *m*-H, ³J_{HH} = 7.86 Hz), 7.63 (d, 8H, arom. *o*-H, ³J_{HH} = 7.86 Hz). ¹³C

NMR (DMSO-d₆; 151 MHz; δ, ppm): 21.16 (−CH₃), 102.41 (CN), 124.69 (C_i), 130.97 (C_m), 135.04 (s, C_o), 142.68 (C_p).

For C₃₀H₂₈N₂I₂SbAu

Anal. calcd., %	C, 36.43	H, 2.86
Found, %	C, 36.39	H, 2.90

Compounds **II** and **III** were synthesized by a similar procedure.

II: dark red crystals, 96% yield, $T_m = 143^\circ\text{C}$.

IR (ν, cm^{−1}): 3049, 2991, 2978, 2908, 2164, 1585, 1483, 1436, 1334, 1321, 1190, 1159, 1112, 1028, 997, 923, 910, 850, 786, 744, 719, 688, 503, 491, 443, 432, 418.

¹H NMR (DMSO-d₆; 600 MHz; δ, ppm): 3.15 (d, 3H, $J_{\text{H}-\text{P}} = 14.61$ Hz, −CH₃), 7.79–7.76 (m, 12H, arom. *m*- and *o*-H), 7.91–7.89 (m, 3H, arom. *p*-H). ¹³C NMR (DMSO-d₆; 151 MHz; δ, ppm): 7.26 (d, CH₃, $J_{\text{C}-\text{P}} = 56.07$ Hz), 102.45 (CN), 119.86 (d, C_i, $J_{\text{C}-\text{P}} = 88.17$ Hz), 130.10 (d, C_o, $J_{\text{C}-\text{P}} = 13.00$ Hz), 133.22 (d, C_m, $J_{\text{C}-\text{P}} = 10.75$ Hz), 134.82 (d, C_p, $J_{\text{C}-\text{P}} = 3.16$ Hz).

For C₂₁H₁₈N₂PI₂Au

Anal. calcd., %	C, 32.33	H, 2.33
Found, %	C, 32.28	H, 2.42

III: dark red crystals, 93% yield, $T_m = 128^\circ\text{C}$.

IR (ν, cm^{−1}): 3059, 2900, 2866, 2254, 2160, 1585, 1483, 1436, 1382, 1342, 1317, 1247, 1236, 1188, 1163, 1111, 1026, 995, 842, 827, 771, 752, 740, 719, 688, 549, 499, 493, 459, 445, 420.

¹H NMR (DMSO-d₆; 600 MHz; δ, ppm): 5.70 (d, 2H, $J_{\text{H}-\text{P}} = 15.87$ Hz, −CH₂CN), 7.87–7.83 (m, 12H, arom. *m*- and *o*-H), 8.02–8.00 (m, 9H, arom. *p*-H). ¹³C NMR (DMSO-d₆; 151 MHz; δ, ppm): 14.04 (d, C-7, $J_{\text{C}-\text{P}} = 55.05$ Hz), 102.45 (CN), 112.78 (d, CN, $J_{\text{C}-\text{P}} = 9.06$ Hz), 116.11 (d, C_i, $J_{\text{C}-\text{P}} = 88.64$ Hz), 130.65 (d, C_o, $J_{\text{C}-\text{P}} = 13.42$ Hz), 133.75 (d, C_m, $J_{\text{C}-\text{P}} = 11.01$ Hz), 136.11 (d, C_p, $J_{\text{C}-\text{P}} = 3.07$ Hz).

For C₂₂H₁₇N₃PI₂Au

Anal. calcd., %	C, 32.82	H, 2.13
Found, %	C, 32.78	H, 2.23

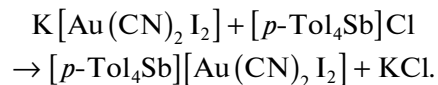
IR spectra of complexes **I**–**III** were measured on a Shimadzu IR Affinity-1S IR spectrometer in the 4000–400 cm^{−1} range (KBr pellets). ¹H (600 MHz) and ¹³C NMR (151 MHz) spectra were recorded on a Bruker AVANCE NEO NMR spectrometer in DMSO-d₆. For ¹H and ¹³C NMR spectra, solvent signals were used as the internal standards.

Single crystal X-ray diffraction study of **I**–**III** was carried out using a D8 Quest Bruker diffractometer (MoK_α radiation, $\lambda = 0.71073$ Å, graphite monochromator) at 293 K. The SMART and SAINT-Plus software was used for data collection and editing, refinement of unit cell parameters, and applying absorption corrections [21]. All calculations for structure determination and refinement were carried out using the SHELXL/PC [22] and OLEX2 [23] software. The structures were determined by direct methods and refined by the least squares method in the anisotropic approximation for non-hydrogen atoms. Hydrogen atom positions were determined geometrically using the riding model. The crystallographic data and structure refinement details are summarized in Table 1 and the key bond lengths and bond angles are given in Table 2.

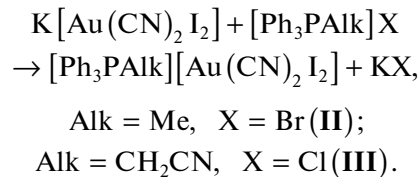
The full tables of atom coordinates, bond lengths, and bond angles are deposited with the Cambridge Crystallographic Data Centre (CIF files CCDC no. 1901681 (**I**), 1912903 (**II**), 1912919 (**III**); deposit@ccdc.cam.ac.uk; <http://www.ccdc.cam.ac.uk/structures>).

RESULTS AND DISCUSSION

Complex **I** was synthesized from potassium dicyanodiiodoaurate and tetra(*para*-tolyl)antimony chloride in aqueous solution:



Complexes **II** and **III** containing organophosphorus cations were prepared by a similar procedure from potassium dicyanodiiodoaurate and alkyltriphenylphosphonium bromide or chloride, respectively:



Evaporation of water, drying of the solid residue, and recrystallization from an acetonitrile and ethanol mixture gave air-stable red crystals.

IR spectroscopy is a reliable method for identifying organic compounds containing a cyano group, since the absorption range of this group is fairly narrow (2200 to 2000 cm^{−1}) [24]. Therefore, cyanides can easily be identified by the presence of a medium-intensity band in this range. The C≡N stretching bands were found at 2156, 2164, and 2160 cm^{−1} in the spectra of compounds **I**, **II**, and **III**, respectively. The IR spectrum of compound **I** shows an intense band for the Sb–C stretching mode at 480 cm^{−1}; asymmetric and symmetric stretching modes of methyl groups occur at 2916 and 2862 cm^{−1}, respectively. The P–Ph absorp-

Table 1. Crystallographic data and X-ray experiment and structure refinement details for structures **I**–**III**

Parameter	Value		
	I	II	III
<i>M</i>	989.06	780.11	805.12
System	Monoclinic	Monoclinic	Triclinic
<i>T</i> , K	293.15	293.15	293.15
Space group	<i>P</i> 2 ₁ /c	<i>P</i> 2 ₁ /c	<i>P</i> 1̄
<i>a</i> , Å	12.870(7)	11.225(6)	8.681(3)
<i>b</i> , Å	15.510(6)	12.300(4)	12.433(7)
<i>c</i> , Å	16.600(6)	17.280(5)	13.016(6)
α, deg	90.00	90.00	66.61(2)
β, deg	104.91(2)	92.764(17)	84.32(2)
γ, deg	90.00	90.00	70.89(2)
<i>V</i> , Å ³	3202(3)	2383.0(16)	1217.5(10)
<i>Z</i>	4	4	2
ρ(calcd.), g/cm ³	2.051	2.174	2.196
μ, mm ⁻¹	7.367	8.840	8.656
<i>F</i> (000)	1832.0	1432.0	740.0
Crystal size, mm	0.23 × 0.18 × 0.15	0.3 × 0.15 × 0.08	0.22 × 0.19 × 0.12
2θ, deg	5.72–58.54	6.62–67.58	5.92–80.7
Ranges of reflection indices	–17 ≤ <i>h</i> ≤ 17, –21 ≤ <i>k</i> ≤ 21, –22 ≤ <i>l</i> ≤ 22	–17 ≤ <i>h</i> ≤ 17, –18 ≤ <i>k</i> ≤ 19, –27 ≤ <i>l</i> ≤ 26	–15 ≤ <i>h</i> ≤ 15, –22 ≤ <i>k</i> ≤ 22, –23 ≤ <i>l</i> ≤ 23
Total number of reflections	78498	88941	103809
Number of unique reflections	8664	9510	15357
Reflections with <i>I</i> > 2σ(<i>I</i>)	(<i>R</i> _{int} = 0.0422)	(<i>R</i> _{int} = 0.0438)	(<i>R</i> _{int} = 0.0623)
Number of refined parameters	329	245	265
GOOF	1.040	1.009	1.008
<i>R</i> -factors on <i>F</i> ² > 2σ(<i>F</i> ²)	<i>R</i> ₁ = 0.0490, <i>wR</i> ₂ = 0.1136	<i>R</i> ₁ = 0.0440, <i>wR</i> ₂ = 0.0917	<i>R</i> ₁ = 0.0530, <i>wR</i> ₂ = 0.0806
<i>R</i> -factors for all reflections	<i>R</i> ₁ = 0.0719, <i>wR</i> ₂ = 0.1286	<i>R</i> ₁ = 0.0849, <i>wR</i> ₂ = 0.1084	<i>R</i> ₁ = 0.1465, <i>wR</i> ₂ = 0.1000
Residual electron density (max/min), e/Å ³	3.56/–2.96	2.29/–2.55	1.36/–1.50

tion band in the spectra of compounds **II** and **III** is observed at 1436 cm^{–1} in both cases, which is in line with the absorption region of 1450–1435 cm^{–1} reported in [24].

The ¹H NMR spectrum of compound **I** shows doublets for the *m*- and *o*-protons at 7.48 and 7.63 ppm, respectively, and a singlet for the methyl group at 2.41 ppm, which are typical of the tolyl moiety. The proton signals of the benzene rings of alkyltriphenylphosphonium complexes include multiplets for the *p*-protons at 7.91–7.89 (**II**) and 8.02–8.00 (**III**) ppm and for the *m*- and *o*-protons at 7.79–7.76 (**II**) and 7.87–7.83 (**III**) ppm. The alkyl group protons for complexes **II** and **III** are manifested in the ¹H NMR

spectra as doublets at 3.15 and 5.70 ppm due to spin–spin coupling with phosphorus, with the coupling constants being 14.61 and 15.87 Hz, respectively. In the ¹³C NMR spectrum of complex **I**, all signals occur as singlets, while the ¹³C NMR spectra of complexes **II** and **III** exhibit doublets due to spin–spin coupling with phosphorus, characterized by the corresponding constants. The cyano group carbon gives rise to signals at 102.41 (**I**), 102.45 (**II**), and 102.45 (**III**) ppm. The carbon signal for the cyano group at the cation is a doublet at 112.78 ppm with the spin–spin coupling constant of 9.06 Hz.

According to X-ray diffraction data, compounds **I**–**III** are ionic complexes with a tetrahedral coordina-

Table 2. Selected bond lengths and bond angles in structures I–III*

Bond	Length, Å	Angle	ω, deg
I			
Au(1)–I(1)	2.6112(10)	I(2)Au(1)I(1)	176.88(3)
Au(1)–I(2)	2.5977(10)	C(8)Au(1)I(1)	89.6(3)
Au(1)–C(8)	2.001(8)	C(8)Au(1)I(2)	90.2(3)
Au(1)–C(9)	1.999(9)	C(9)Au(1)I(1)	91.1(2)
Sb(1)–C(1)	2.084(7)	C(9)Au(1)I(2)	89.1(2)
Sb(1)–C(21)	2.088(7)	C(9)Au(1)C(8)	179.2(4)
Sb(1)–C(31)	2.093(8)	C(1)Sb(1)C(21)	109.2(3)
Sb(1)–C(11)	2.098(8)	C(1)Sb(1)C(31)	109.8(3)
N(1)–C(8)	1.133(11)	C(1)Sb(1)C(11)	109.9(3)
N(2)–C(9)	1.133(11)	C(21)Sb(1)C(31)	106.4(3)
C(34)–C(37)	1.526(14)	C(21)Sb(1)C(11)	112.5(3)
C(4)–C(7)	1.497(10)	C(31)Sb(1)C(11)	108.9(3)
II			
Au(1)–I(1)	2.6030(8)	I(1)Au(1)I(2)	177.656(18)
Au(1)–I(2)	2.6118(7)	C(9)Au(1)I(1)	90.92(16)
Au(1)–C(9)	2.002(6)	C(9)Au(1)I(2)	91.38(16)
Au(1)–C(8)	2.026(6)	C(9)Au(1)C(8)	178.7(2)
P(1)–C(11)	1.796(4)	C(8)Au(1)I(1)	88.33(16)
P(1)–C(21)	1.787(5)	C(8)Au(1)I(2)	89.38(16)
P(1)–C(1)	1.798(5)	C(11)P(1)C(1)	108.4(2)
P(1)–C(7)	1.791(5)	C(21)P(1)C(11)	110.8(2)
N(2)–C(9)	1.132(7)	C(21)P(1)C(1)	109.4(2)
N(1)–C(8)	1.075(8)	C(21)P(1)C(7)	108.5(2)
C(4)–C(3)	1.364(10)	C(7)P(1)C(11)	109.9(2)
C(1)–C(2)	1.379(7)	C(7)P(1)C(1)	109.9(3)
III			
Au(1)–I(1) ¹	2.6199(11)	I(1) ¹ Au(1)I(1)	180.000(14)
Au(1)–I(1)	2.6199(11)	C(9) ¹ Au(1)I(1) ¹	90.51(12)
Au(1)–C(9)	2.004(4)	C(9)Au(1)I(1) ¹	89.49(12)
Au(1)–C(9) ¹	2.004(4)	C(9) ¹ Au(1)I(1)	89.49(12)
Au(2)–I(2) ²	2.6194(11)	C(9)Au(1)I(1)	90.51(12)
Au(2)–I(2)	2.6194(11)	C(9) ¹ Au(1)C(9)	180.0
Au(2)–C(10)	2.008(4)	I(2) ² Au(2)I(2)	180.0
Au(2)–C(10) ²	2.008(4)	C(10) ² Au(2)I(2) ²	90.30(12)
P(1)–C(11)	1.790(3)	C(10)Au(2)I(2) ²	89.70(12)
P(1)–C(1)	1.781(3)	C(10) ² Au(2)I(2)	89.70(12)
P(1)–C(21)	1.786(3)	C(10)u(2)I(2)	90.30(12)
P(1)–C(7)	1.826(3)	C(10)Au(2)C(10) ²	179.999(1)
N(1)–C(9)	1.137(5)	C(11)P(1)C(7)	110.26(16)
N(3)–C(8)	1.137(5)	C(1)P(1)C(11)	108.76(16)
N(2)–C(10)	1.120(5)	C(1)P(1)C(21)	110.21(15)
C(7)–C(8)	1.452(5)	C(1)P(1)C(7)	110.41(16)
C(2)–C(1)	1.388(5)	C(21)P(1)C(11)	111.65(15)
C(1)–C(6)	1.379(5)	C(21)P(1)C(7)	105.53(16)

* Symmetry codes: ¹ $-x, -y, 1 - z$; ² $-x, 2 - y, -z$.

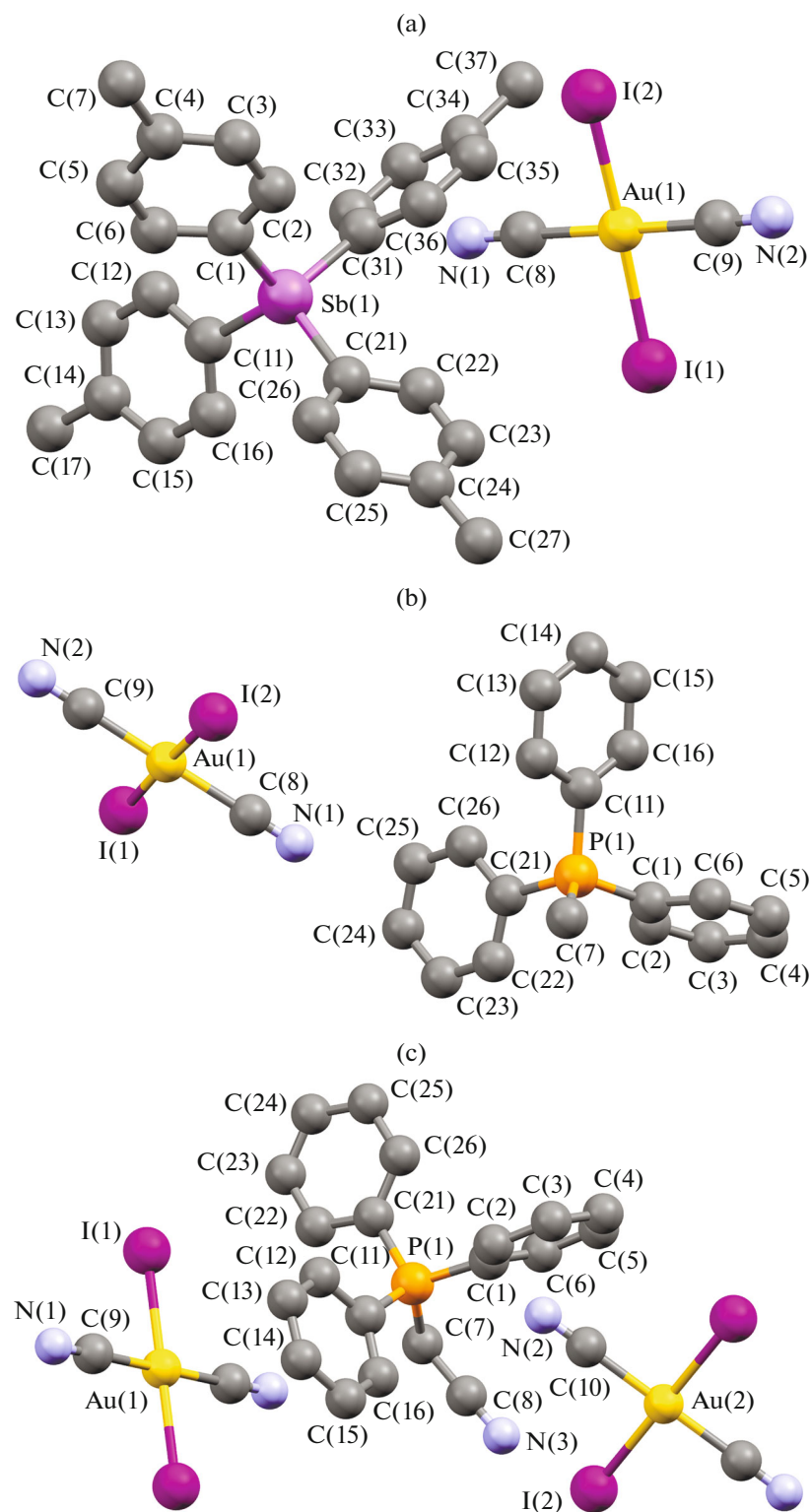


Fig. 1. General view of complexes (a) I, (b) II, and (c) III.

tion of the central atom in the cation and a planar dicyanodiiodoaurate anion. The crystal of **III** contains two types of centrosymmetrical crystallographically independent dicyanodiiodoaurate anions (Fig. 1).

The tetrahedral coordinations of antimony atoms in the cation of **I** and phosphorus atoms in **II** and **III** are distorted to a minor extent. The CSbC or CPC angles deviate from the theoretical value, varying in

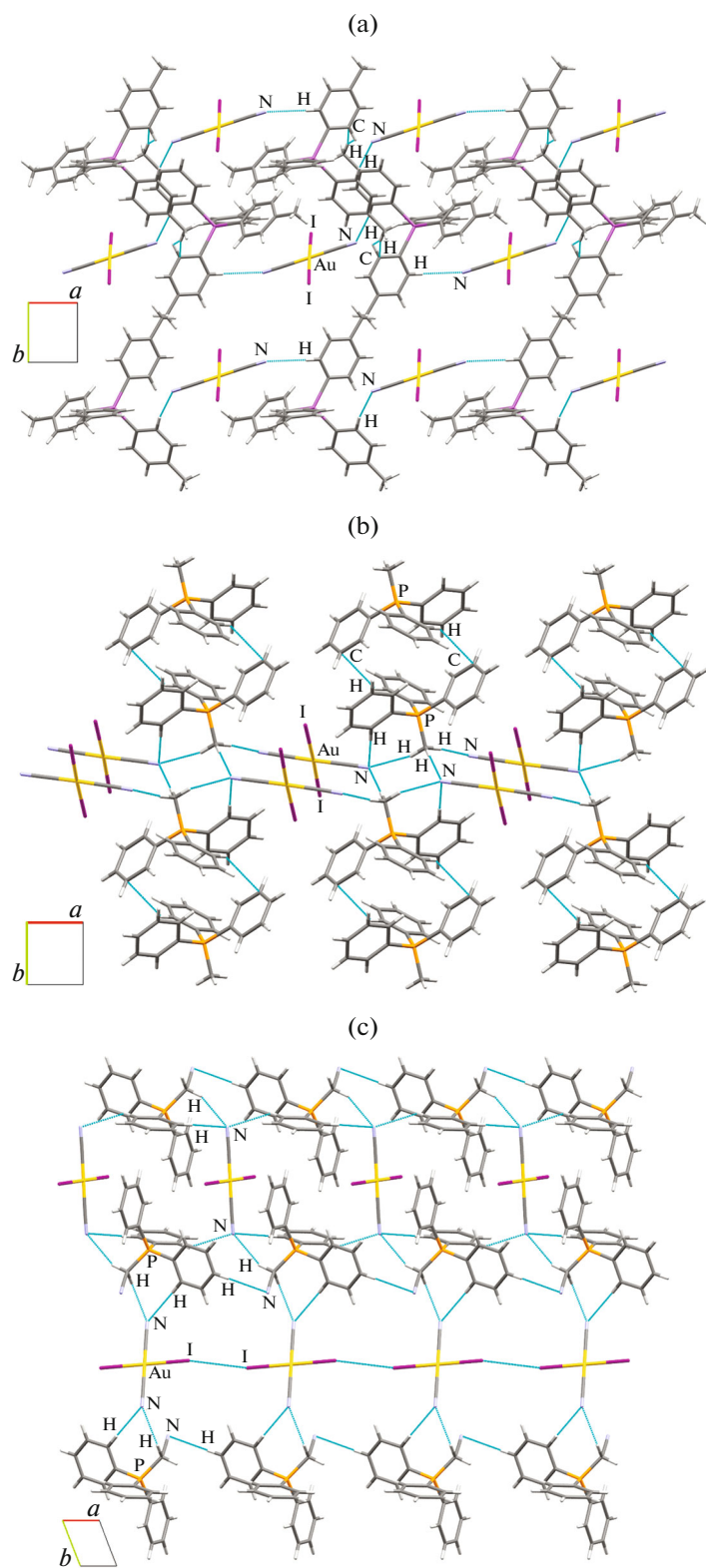


Fig. 2. Interactions between ions of complexes (a) I, (b) II, and (c) III. View from the *ab* plane.

the ranges of $106.4(3)^\circ$ – $112.5(3)^\circ$ (**I**), $108.4(2)^\circ$ – $110.8(2)^\circ$ (**II**), and $105.53(16)^\circ$ – $111.65(15)^\circ$ (**III**). In the tetra(*para*-tolyl)antimony cation, the average Sb–C bond length is $2.091(8)$ Å. In the organophosphorus cation of complex **II**, the P–C distances differ little irrespective of the nature of the substituent ($1.796(4)$ (Ph), $1.787(5)$ (Ph), $1.798(5)$ (Ph), and $1.791(5)$ (CH_3) Å). The presence of the cyano group in the cation of **III** accounts for the longer P–C_{Alk} bond length ($1.826(3)$ Å) compared with the P–C_{Ph} length ($1.790(3)$, $1.781(3)$, $1.786(3)$ Å). The $[\text{Au}(\text{CN})_2\text{I}_2]^-$ square anions slightly deviate from planarity, the CAuC angles being $179.2(4)^\circ$ (**I**), $178.7(2)^\circ$ (**II**), and 180.0° , $179.999(1)^\circ$ (**III**). The Au–C distances in the anions of **I**, **II**, and **III** are shorter than the sum of the covalent radii of gold and carbon atoms (2.03 Å [25]), being $2.001(8)$, $1.999(9)$ Å (**I**), $2.002(6)$, $2.026(6)$ Å (**II**), and $2.004(4)$, $2.004(4)$ and $2.008(4)$, $2.008(4)$ Å (**III**), respectively. The Au–I bond lengths are $2.6112(10)$, $2.5977(10)$ Å (**I**), $2.6030(8)$, $2.6118(7)$ Å (**II**), and $2.6199(11)$, $2.6194(11)$ Å (**III**).

The 3D crystal network is formed by weak $\text{CN}\cdots\text{H}=\text{C}$ hydrogen bonds between the cations and anions (2.39 , 2.59 Å (**I**), 2.70 , 2.48 , 2.52 , 2.68 Å (**II**), 2.73 , 2.50 , 2.67 , 2.44 Å (**III**)). The cations of **I** and **II** are connected by C–H $\cdots\pi$ -interactions, with the distances from hydrogen atom to the benzene ring plane being 2.77 and 2.82 Å, respectively (Figs. 2a, 2b). The cations of **III** are connected via C_{Ph}–H $\cdots\text{NC}_{\text{Alk}}$ hydrogen bonds (2.72 Å). In this complex, anions of one of the two types also interact with one another via I \cdots I contacts, giving rise to 1D chains along the crystallographic *a* axis (Fig. 2c). The I \cdots I distances are shorter than twice the van der Waals radius of iodine (4.30 Å) and amount to 3.93 Å, which is indicative of halogen \cdots halogen contacts. As shown in Fig. 2c, anions of one of the two types are arranged in such a way that iodine ligands form a ladder-like chain. This, in turn, results in parallel alignment of the $[\text{Au}(\text{CN})_2\text{I}_2]^-$ groups along the crystallographic *a* axis. The Au–I \cdots I angles between the connected pairs of anions are 141.90° , which provides for the ladder motif. This I \cdots I interaction refers to type I, since the difference between the Au–I \cdots I angles is 0° [26].

Thus, tetra(*para*-tolyl)antimony and alkyltriphenylphosphonium dicyanodiiodoaurate complexes prepared from the corresponding alkyltriphenylphosphonium, tetra(*para*-tolyl)antimony halides and potassium dicyanodiiodoaurate in water are ionic compounds with monomeric dicyanodiiodoaurate anions. The structural organization of complex **III** is due not only to hydrogen bonds involving the cyano group, as in other complexes, but also to halogen–halogen interactions between the iodine atoms.

CONFLICT OF INTEREST

The authors declare that they have no conflicts of interest.

FUNDING

This study was supported by the Ministry of Education and Science of the Russian Federation (grant no. 4.6151.2017/8.9).

REFERENCES

1. Xiaobo, L. and Patterson, H., *Materials*, 2013, vol. 6, p. 2595.
<https://doi.org/10.3390/ma6072595>
2. Dechambenoit, P., Ferlay, S., Kyritsakas, N., et al., *CrystEngComm*, 2011, vol. 13, p. 1922.
<https://doi.org/10.1039/C0CE00607F>
3. Hill, J.A., Thompson, A.L., and Goodwin, A.L., *J. Am. Chem. Soc.*, 2018, vol. 138, p. 5886.
<https://doi.org/10.1021/jacs.5b13446>
4. Assefa, Z., Haire, R.G., and Sykora, R.E., *J. Solid State Chem.*, 2008, vol. 181, p. 382.
<https://doi.org/10.1016/j.jssc.2007.11.036>
5. Brown, M.L., Ovens, J.S., and Leznoff, D.B., *Dalton Trans.*, 2017, vol. 46, p. 7169.
<https://doi.org/10.1039/C7DT00942A>
6. Chorazy, S., Wyczesany, M., and Sieklucka, B., *Molecules*, 2017, vol. 22, p. 1902.
<https://doi.org/10.3390/molecules22111902>
7. Shaw, C.F., *Chem. Rev.*, 1999, vol. 99, no. 9, p. 2589.
<https://doi.org/10.1021/cr980431o>
8. Roberts, R.J., Le, D., and Leznoff, D.B., *Inorg. Chem.*, 2017, vol. 56, no. 14, p. 7948.
<https://doi.org/10.1021/acs.inorgchem.7b00735>
9. Rawashdeh-Omary, M.A., Omary, M.A., Shankle, G.E., et al., *J. Phys. Chem. B*, 2000, vol. 104, no. 26, p. 6143.
<https://doi.org/10.1021/jp000563x>
10. Colis, J.C.F., Larochelle, C., Fernández, E.J., et al., *J. Phys. Chem. B*, 2005, vol. 109, no. 10, p. 4317.
<https://doi.org/10.1021/jp045868g>
11. Assefa, Z., Kalachnikova, K., Hairec, R.G., et al., *J. Solid State Chem.*, 2007, vol. 180, p. 3121.
<https://doi.org/10.1016/j.jssc.2007.08.032>
12. Ovens, J.S. and Leznoff, D.B., *Chem. Mater.*, 2015, vol. 27, no. 5, p. 1465.
<https://doi.org/10.1021/cm502998w>
13. Ovens, J.S. and Leznoff, D.B., *Dalton Trans.*, 2011, p. 4140.
<https://doi.org/10.1039/c0dt01772h>
14. Sharutin, V.V., Popkova, M.A., and Tarasova, N.M., *Bull. South Ural State Univ., Ser. Chem.*, 2018, vol. 10, no. 1, p. 55.
<https://doi.org/10.14529/chem180107>
15. Sharutin, V.V., Sharutina, O.K., and Popkova, M.A., *Russ. J. Inorg. Chem.*, 2019, vol. 64, no. 6, p. 607.
<https://doi.org/10.1134/S0036023619060147>
16. Cambridge Crystallographic Data Center, 2018.
<http://www.ccdc.cam.ac.uk>.

17. Ovens, J.S., Geisheimer, A.R., Bokov, A.A., et al., *Inorg. Chem.*, 2010, vol. 49, p. 9609.
<https://doi.org/10.1021/ic101357y>
18. Pitteri, B., Bortoluzzi, M., and Bertolasi, V., *Transition Met. Chem.*, 2008, vol. 33, p. 649.
<https://doi.org/10.1007/s11243-008-9092-9>
19. Marangoni, G., Pitteri, B., Bertolasi, V., et al., *Dalton Trans.*, 1987, no. 1, p. 2235.
<https://doi.org/10.1039/DT9870002235>
20. Ovens, J.S., Truong, K.N., and Leznoff, D.B., *Dalton Trans.*, 2012, vol. 41, p. 1345.
<https://doi.org/10.1039/c1dt11741f>
21. *SMART and SAINT-Plus. Versions 5.0. Data Collection and Processing Software for the SMART System*, Madison: Bruker AXS Inc., 1998.
22. *SHELXTL/PC. Versions 5.10. An Integrated System for Solving, Refining and Displaying Crystal Structures from Diffraction Data*, Madison: Bruker AXS Inc., 1998.
23. Dolomanov, O.V., Bourhis, L.J., Gildea, R.J., et al., *J. Appl. Crystallogr.*, 2009, vol. 42, p. 339.
<https://doi.org/10.1107/S0021889808042726>
24. Pretsch, E., Bühlmann, F., and Affolter, C., *Structure Determination of Organic Compounds*, Berlin: Springer, 2000.
25. Batsanov, S.S., *Russ. J. Inorg. Chem.*, 1991, vol. 3, p. 1694.
26. Mukherjee, A., Tothadi, S., and Desiraju, G.R., *Acc. Chem. Res.*, 2014, vol. 47, no. 8, p. 2514.
<https://doi.org/10.1021/ar5001555>

Translated by Z. Svitanko